EMITTER International Journal of Engineering Technology
Vol. 13, No. 1, June 2025, pp. 56~72
DOI : 10.24003/emitter.v13i1.892

Synergistic Integration of LQR Control and PSO Optimization for Advanced Active Suspension Systems Utilizing Electro-Hydraulic Actuators and Electro-Servo Valves

Do Trong Tu[1]

[1]Faculty of Mechanical - Automotive and Civil Engineering, Electric Power University, Hanoi, Vietnam.
Corresponding Author: tudt@epu.edu.vn

Received February 5, 2025; Revised March 10, 2025; Accepted April 22, 2025

Abstract

This paper investigates the design and optimization of Linear Quadratic Regulator (LQR) controllers for vehicle active suspension systems, incorporating an electro-hydraulic actuator with an electro-servo valve. To enhance both vehicle comfort and road-holding stability, we employ Particle Swarm Optimization (PSO) to optimize the LQR controller parameters. The active suspension system model includes the dynamics of the electro-hydraulic actuator and the electro-servo valve, providing a realistic and practical framework for heavy vehicles. By leveraging PSO, the LQR controller parameters are fine-tuned to minimize a cost function that integrates both comfort and stability up to 76.91%. The results demonstrate substantial improvements in ride comfort and road-holding stability compared to traditional passive suspension systems. This research remarks the fundamentals of the experimental validation and further refinement of these control algorithms to adapt to various driving conditions and vehicle models, ultimately aiming to transition these optimized controllers from theoretical frameworks to practical, real-world applications.

Keywords: active suspension system, electro-hydraulic actuator, vehicle comfort, road holding, vehicle vibration, particle swarm optimization, linear quadratic regulator

1. INTRODUCTION

The evolution of vehicle suspension systems on heavy vehicles from passive to active has been a significant area of research and development in automotive engineering. Passive suspension systems, which rely on fixed parameters to manage vehicle dynamics, have inherent limitations in adaptability and performance optimization under varying road conditions [1], [2], [3]. These limitations have prompted extensive research into active suspension systems, which can dynamically adjust to changing conditions, thereby offering improved ride quality and handling. Active suspension systems play a crucial role in modern vehicle dynamics, significantly influencing ride comfort and road-holding stability. Traditional passive suspension systems, although widely used, often present a trade-off between comfort and stability, as they cannot adapt to varying road conditions and driving scenarios. To address these limitations, active suspension systems with advanced actuators as well as control strategies have emerged as a promising solution [4], [5], [6].

2. RELATED WORKS

An active suspension system utilizing an electro-hydraulic actuator as a high-efficiency damper significantly enhances vehicle performance by dynamically adjusting to road conditions in real time [7], [8]. This advanced setup leverages precise electronic control combined with hydraulic power to modulate suspension stiffness and damping characteristics instantaneously. This ensures optimal tire contact with the road, improving ride comfort, handling, and safety. The electro-hydraulic actuator’s rapid response capabilities allow for fine-tuned adjustments, reducing body roll, pitch, and heave, thereby delivering a smoother and more stable driving experience across diverse terrains and driving scenarios [9]. Incorporating electro-hydraulic actuators and electro-servo valves into active suspension systems has been another focus area [10]. These components provide precise control capabilities necessary for fine adjustments in suspension dynamics. Researchers like [11], [12] have demonstrated the effectiveness of electro-hydraulic systems in enhancing vehicle ride and stability. Their work underscores the importance of accurately modeling these components to achieve realistic and practical solutions.

Besides that, the controller's technique impacts the effectiveness for the suspension that is active technology [13]. The Linear Quadratic Regulator (LQR) controller is highly effective for active suspension systems, offering optimal control by minimizing a quadratic cost function, but its design demands complex and time-intensive parameter tuning to balance comfort and stability. Recent studies have explored different methods to address the tuning of LQR parameters. Several robust and efficient optimization techniques inspired by the social behaviors of bird flocking and fish schooling have been deployed to search for the optimal weighting parameters for the LQR controller [14], [15]. Saptarshi [16] employed a multi-objective optimization approach to fine-tune LQR weights, highlighting the trade-offs between various performance criteria. In addition, [17] investigated the use of genetic algorithms to optimize LQR controller parameters for a quarter-car active suspension model, demonstrating notable improvements in performance metrics. Particle Swarm Optimization (PSO) has emerged as a powerful optimization technique for tuning control parameters in complex systems [18], [19]. The proposed technique improves PSO by adaptively updating inertia weight based on particle success rates to enhance convergence and incorporating a predator–prey strategy to prevent premature convergence and ensure global optimality [20]. The researchers [21], [22] introduced PSO, inspired by the social behaviors patterns of birds and fish, as an efficient method for solving nonlinear optimization problems. In the context of active suspension systems, PSO has been utilized to optimize control parameters, showing promising results. Li et. al [23] applied PSO to optimize fuzzy logic controllers for active suspension systems, achieving significant improvements in ride comfort and stability. By using PSO, the LQR controller parameters achieve a balanced improvement in both vehicle comfort and road-holding stability [24]. The swarm optimization-based LQR-PID controller, tested on a four-degree-of-freedom model outperforms LQR and LQR-PID controllers optimized by Swarm Optimization techniques [25], [26].

3. ORIGINALITY

This paper expands on the existing body of knowledge by integrating LQR control with PSO optimization for an active suspension system model that includes electro-hydraulic actuators and electro-servo valves. Our objective is to offer a comprehensive and practical approach to enhancing vehicle dynamics, significantly improving upon traditional passive systems. We investigate the design and optimization of LQR controllers for vehicle active suspension systems, incorporating electro-hydraulic actuators with electro-servo valves. Including these components adds realism and practicality to the suspension model, particularly for heavy vehicles where such systems are commonly employed.

4. SYSTEM DESIGN

4.1 Quarter-heavy vehicle modeling

A quarter-heavy vehicle model represents a single corner of a heavy vehicle with two degrees of freedom, as shown in Figure 1. This model, which contains the vertical chassis and wheel bounce displacement, allows studying only the vertical dynamic behavior of the heavy vehicle. This simple model consists of the sprung mass m_s represents a quarter of the vehicle body. The unsprung mass m_u represents the wheel and the tire of the vehicle. Z_s, Z_u stand for the vertical displacement of the sprung mass and unsprung mass, respectively. The suspension mechanism involves an elastic spring whose stiffness coefficient k_s and a damper with it's passive damping coefficient c_s. The wheel is represented by an elastic spring whose stiffness coefficient k_t, the vertical disturbance of the road's profile q.

The dynamic equations of the system around the equilibrium can be derived using Newton's second law of motion.

$$\begin{cases} m_s\ddot{z}_s = -k_s(z_s - z_u) - c_s(\dot{z}_s - \dot{z}_u) - F_{act} \\ m_u\ddot{z}_u = k_s(z_s - z_u) + c_s(\dot{z}_s - \dot{z}_u) - k_t(z_u - q) + F_{act} \end{cases} \tag{1}$$

A high-pressure oil is perpetually kept in reservoir and distributes among the hydraulic cylinder's two chambers cause difference in pressures $\Delta P = P_1 - P_2$ that generates the force as

$$F_{act} = A_P \Delta P \tag{2}$$

As a result, the calculations within every compartment evolve into:

$$\begin{cases} A_p \dfrac{dy_a}{dt} + \dfrac{V_0 + A_p y_a}{\beta_e} \dfrac{dP_1}{dt} = Q_1 - C_{ip}(P_1 - P_2) - C_{ep} P_1 \\ -A_p \dfrac{dy_a}{dt} + \dfrac{V_0 - A_p y_a}{\beta_e} \dfrac{dP_2}{dt} = C_{ip}(P_1 - P_2) - C_{ep} P_2 - Q_2 \end{cases} \tag{3}$$

with the overall leaking percentage in the piston hydraulic cylinder $C_{tp} = 2C_{ip} + C_{ep}$, now it becomes.

$$2Q_L = Q_1 + Q_2 = 2C_{tp}\Delta P + 2A_p \frac{dy_a}{dt} + \frac{V_0}{\beta_e} \frac{d\Delta P}{dt} \tag{4}$$

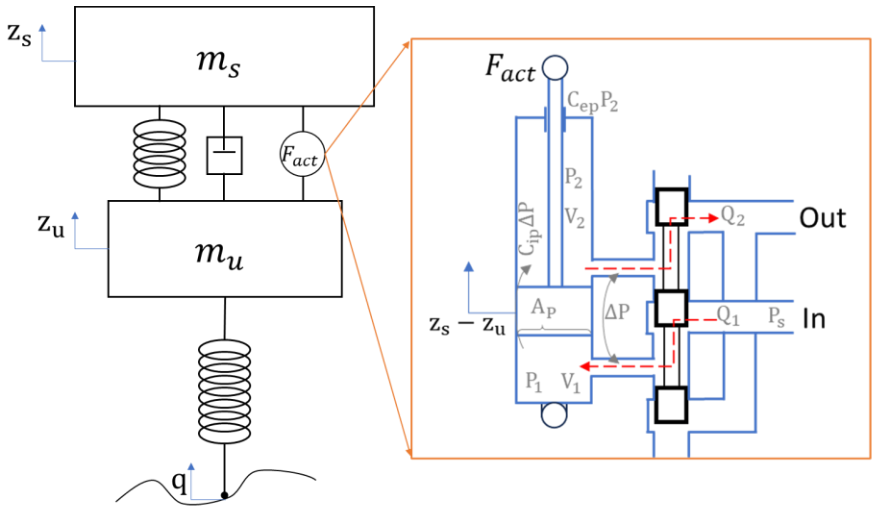

Figure 1. Diagram of the quarter heavy vehicle model with hydraulic electronic servo-valve actuator

By substituting mathematical formulas (3) and (4), the dynamical expression of servo-valve hydraulic pressure cylinder is determined as:

$$\frac{V_t}{4\beta_e} \frac{d\Delta P}{dt} + (K_P + C_{tp})\Delta P - K_x X_v + A_p \frac{d(z_s - z_u)}{dt} = 0 \tag{5}$$

When ignore the inertial and flow forces on the servo-valve, the mechanical behaviour of the electronic servo-valve may be represented by a model of first-order arranged as follows:

$$\frac{dX_v}{dt} + \frac{1}{\tau} X_v - \frac{K_v}{\tau} u = 0 \tag{6}$$

From (1), (2), and (6), the formulation that describes the characteristic of the quarter-heavy vehicle integrated hydraulic electronic servo-valve actuator can be determined as:

$$\begin{cases} m_s \ddot{Z}_s = -k_s(z_s - z_u) - c_s(\dot{z}_s - \dot{z}_u) - A_P \Delta P \\ m_u \ddot{Z}_u = k_s(z_s - z_u) + c_s(\dot{z}_s - \dot{z}_u) - k_t(z_u - q) + A_P \Delta P \\ \dfrac{d\Delta P}{dt} = \dfrac{4\beta_e.A_p}{V_t}(\dot{z}_s - \dot{z}_u) + \dfrac{4\beta_e.(K_P + C_{tp})}{V_t}\Delta P - \dfrac{4\beta_e.K_x}{V_t} X_v \\ \dfrac{dX_v}{dt} - = \dfrac{K_v}{\tau} u_{(v)} - \dfrac{1}{\tau} X_v \end{cases} \tag{7}$$

Table 1. Parameters of the vehicle

Illustrations	Specifications	Value
A_p	The surface surrounding the piston	0.01 m^2
K_x	Valves inflow benefit correlation	2.45 m^2/s
K_P	Maximum pressure inflow factor	42.1×10-12 m^5/Ns
C_{tp}	Maximum actuator's loss rate	0
V_t	Maximum amount oil's absorbed	0.0015 m^3
β_e	The nominal oil's bulk elasticity	6.79×10 6 N/m^2
τ	Temporal constants that control solenoid valves	0.011s
K_v	Servo-valve gains	0.0243 m/A
m_s	Sprung masses	4700 kg
m_u	Unsprung masses	585 kg
c_s	Damper coefficient	25500 N/m
k_s	Suspension stiffening	230000 N/m

4.2 Design the LQR controller-based PSO algorithm

In designing an LQR controller for a 2DOF active suspension system on a heavy vehicle, the objective is to enhance ride comfort and road safety. The suspension system's state-space model includes four key outputs: sprung mass displacement (z_s) and velocity ($\dot{z}_s$), and unsprung mass displacement (z_u) and unsprung mass velocity ($\dot{z}_u$). The system can be described by state-space equations:

$$\begin{cases} \dot{x} = Ax + Bu_o + Ew \\ y = Cx \end{cases} \tag{8}$$

where x represents the state vector encompassing z_s, $\dot{z}_s$, z_u and $\dot{z}_u$; u_o denotes the control input (force from the actuator), and w represents road disturbances. The state-space matrices A, B, E, and C are derived based on the suspension system's dynamics, incorporating stiffness and damping coefficients as well as the dynamic characteristics of the electro-serve valve. The LQR control system attempts to decrease an exponential cost equation specified as:

$$J = \int_0^\infty \left(x^T Q x + u^T R u \right) dt \tag{9}$$

In this formulation, Q is the state weighting matrix and R is the control input weighting matrix. These matrices are crucial for determining the performance of the LQR controller. To find the optimal values for Q and R, the PSO algorithm is utilized. This optimization process seeks to minimize the cost function J while enhancing ride comfort and road safety.

The PSO algorithm involves initializing a population of particles, each representing a potential solution for Q and R. The particles are randomly distributed within the search space . Each particle is evaluated based on the cost function J, which requires simulating the suspension system with the current R and Q values to assess performance metrics related to ride comfort and road safety. The velocity and position of each particle are updated according to (10) [19]:

$$\begin{aligned} v_i(t+1) &= \omega v_i(t) + c_1 r_1 (p_i^{best} - x_i(t)) + c_2 r_2 (g^{best} - x_i(t)) \\ x_i(t+1) &= x_i(t) + v_i(t+1) \end{aligned} \tag{10}$$

where $v_i(t)$ is the velocity of the particle i at time t, $x_i(t)$ is the position of the particle i at time t, p_i^{best} is the best position of the particle i, g^{best} is the best position among all particles, and $\omega = 1, c_1 = 2.4, c_2 = 2.22, r_1 = 0.9, r_2 = 0.9$ are parameters governing the optimization process. The algorithm iterates through these steps until convergence criteria are met or a maximum number of iterations is reached. Once the optimal Q and R matrices are determined, the performance of the LQR controller is validated through simulations. These simulations assess the controller's ability to improve ride comfort and road safety by reducing the sprung mass displacement (z_s) and velocity ($\dot{z}_s$), while also minimizing the impact of road disturbances on the unsprung mass (z_u and $\dot{z}_u$). Performance metrics such as RMS values of z_s and $\dot{z}_s$, and peak values of $\dot{z}_s$ and $\dot{z}_u$ are evaluated to ensure the controller's effectiveness.

The integration of PSO with LQR control for a 2DOF active suspension system in heavy vehicles provides a robust method for optimizing the controller's performance. By fine-tuning the weighting parameters Q and R, this approach achieves significant improvements in ride comfort and road safety, demonstrating its practical applicability for enhancing vehicle dynamics.

5. EXPERIMENT AND ANALYSIS

Figure 2 presents a Pareto plot detailing the optimization process of determining the weighting parameters for the LQR controller using PSO over 500 iterations. Initially, the cost value is approximately 0.095, reflecting the performance of the initial random solutions. As the iterations progress, there is a marked decrease in the cost value, particularly within the first 50 iterations, where the cost value declines significantly to around 0.07. This rapid convergence highlights the PSO algorithm's efficacy in swiftly identifying promising regions within the search space. Between iterations 50 and 150, the cost value exhibits a more gradual decline, eventually stabilizing at approximately 0.065, suggesting that the algorithm is effectively fine-tuning the solutions to enhance performance.

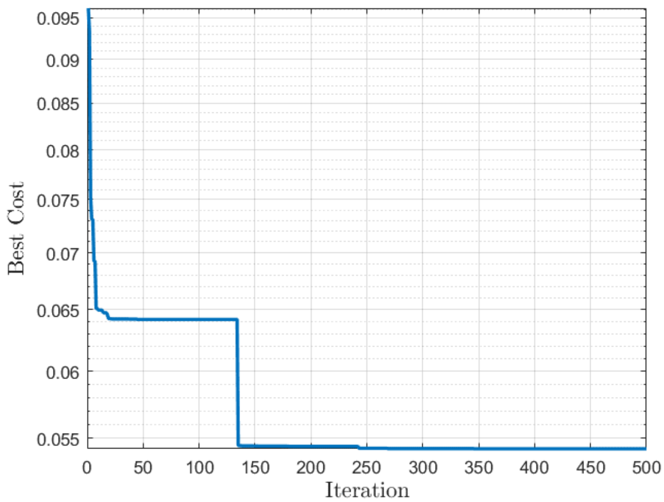

Figure 2. Pareto history of the PSO defined the weighting parameters for the LQR controller

Beyond iteration 150, the cost value experiences a further pronounced reduction to approximately 0.055, where it remains constant for the remainder of the iterations up to 500. This indicates that the PSO algorithm has successfully converged to an optimal or near-optimal solution for the LQR controller's weighting parameters. The stabilization of the cost value beyond this point implies the algorithm's success in optimizing the parameters.

5.1 Analysis in frequency domain results

Figure 3 illustrates the frequency response of a vehicle suspension system using three different control strategies: passive suspension, active LQR, and active PSO-LQR. The passive suspension (blue line) exhibits a prominent resonance peak, indicating reduced effectiveness in vibration dampening. In contrast, the active LQR (red dashed line) consistently stays below the blue line, significantly reducing vibrations and improving ride comfort and road holding. The active PSO-LQR (black dash-dotted line) further enhances performance, particularly around the resonance peak, showcasing the effectiveness of PSO in fine-tuning LQR controller parameters. Both active strategies perform well across the frequency range from 0.1 Hz to 100 Hz, with the PSO-optimized controller offering the best overall performance. This highlights the substantial benefits of using advanced optimization techniques in designing vehicle suspension control systems, emphasizing the potential for improved ride comfort and stability.

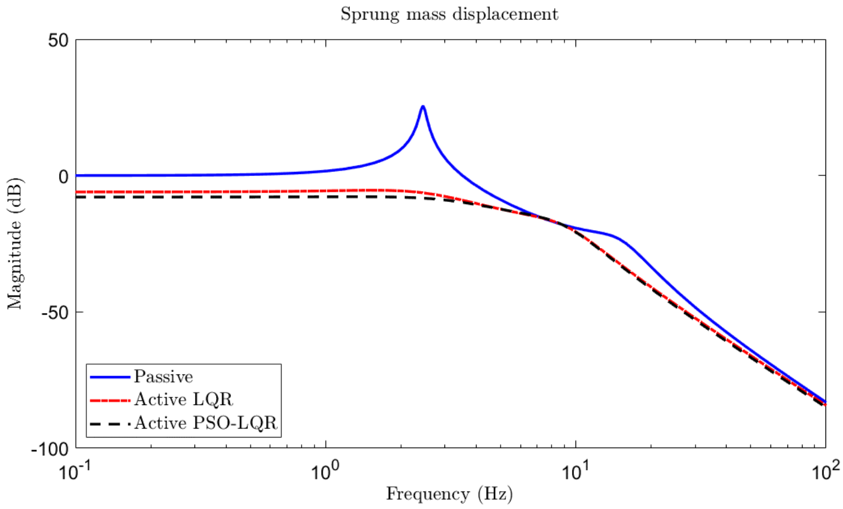

Figure 3. Frequency response of the sprung mass displacement

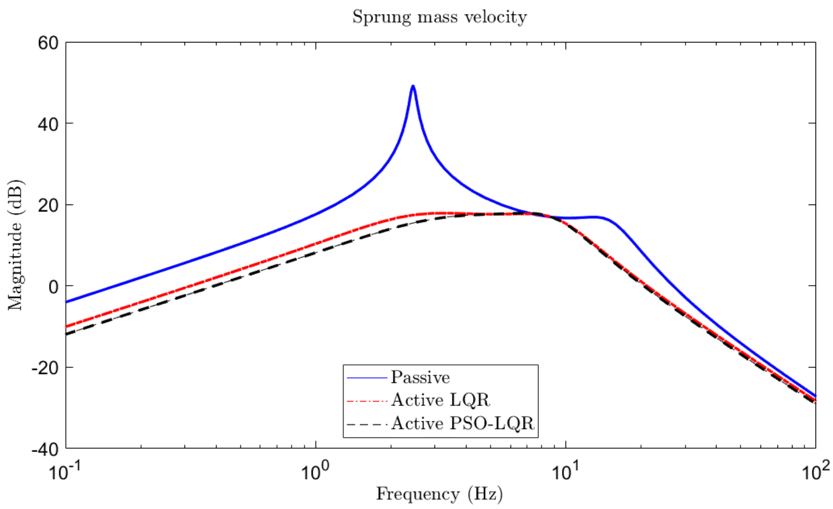

Figure 4. Frequency response of the sprung mass velocity

From Figure 4, it is evident that the passive suspension system exhibits the highest magnitude peak around the resonance frequency, indicating poor performance in terms of ride comfort and road safety. In contrast, both the active LQR and active PSO-LQR systems significantly reduce the magnitude of the sprung mass velocity across the frequency spectrum, with the active PSO-LQR system achieving the lowest peak magnitude. This indicates a more effective suppression of vibrations, leading to enhanced ride comfort and road safety.

The active LQR control shows an improvement over the passive system by lowering the peak response, but the active PSO-LQR control further optimizes this performance. The PSO algorithm's optimization of the LQR controller's weighting parameters results in a more balanced and efficient vibration reduction. Overall, the active PSO-LQR control demonstrates superior performance in minimizing the sprung mass velocity, highlighting its effectiveness in enhancing vehicle dynamics compared to both the passive and conventional active LQR systems.

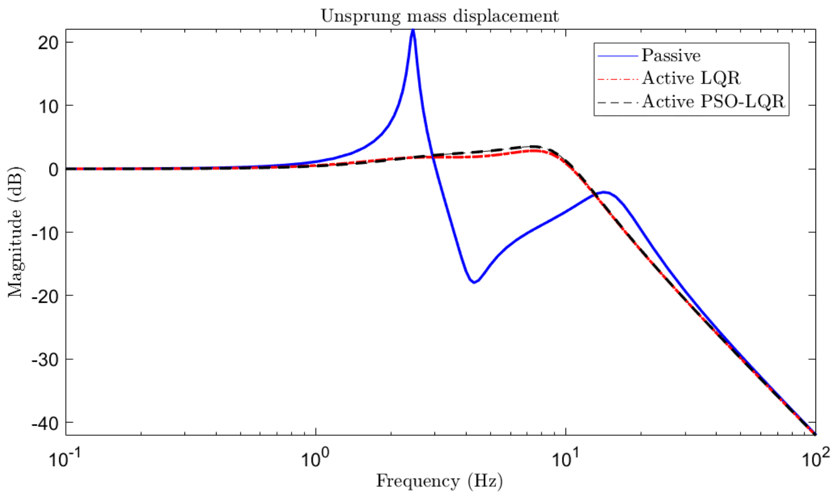

Figure 5. Frequency response of the unsprung mass displacement

The passive suspension system (blue line in Figure 5) shows a significant peak in unsprung mass displacement around the resonance frequency, reaching approximately 18 dB. This peak indicates its inferior performance in mitigating road disturbances, as high displacement magnitudes correspond to poor road handling and increased vibration transfer to the vehicle's chassis. In contrast, both the active LQR (red dotted line in Figure 5) and active PSO-LQR (black dashed line in Figure 5) systems exhibit substantial improvements, reducing the peak magnitude of unsprung mass displacement. The active LQR system lowers the peak to about 10 dB, demonstrating a marked improvement in controlling road-induced vibrations. However, the active PSO-LQR system further optimizes this performance, reducing the peak magnitude to approximately 8 dB, showcasing its superior capability in minimizing displacement compared to both the passive and active LQR systems. While the active LQR control effectively lowers the response compared to the passive system, it does not achieve the same level of performance as the active PSO-LQR control. The PSO algorithm's optimization of the LQR controller's weighting parameters results in a more efficient reduction of unsprung mass displacement across the frequency spectrum. At lower frequencies (around 0.1 Hz to 1 Hz), both active control systems perform similarly, but at higher frequencies (above 1 Hz), the active PSO-LQR control shows a noticeable advantage.

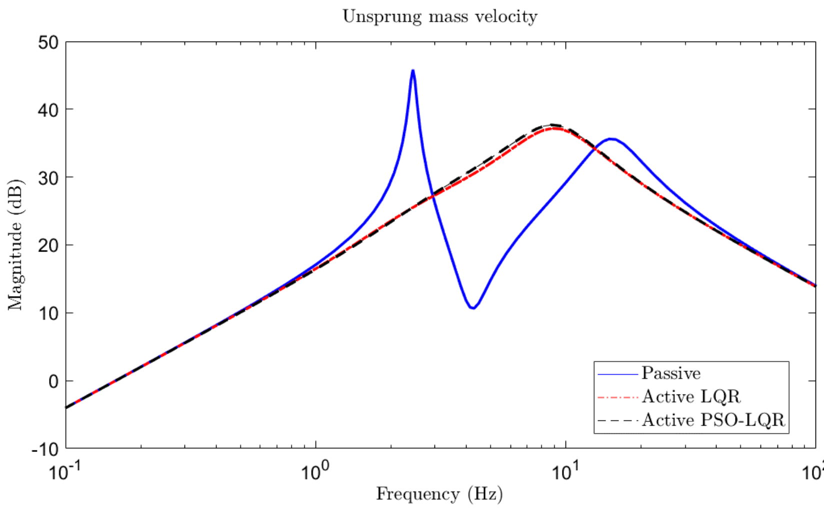

Figure 6. Frequency response of the unsprung mass velocity

Upon Figure 6, the passive suspension system exhibits a pronounced peak in unsprung mass velocity near its resonance frequency, peaking at approximately 42 dB. This peak signifies its limited ability to attenuate disturbances from the road, as higher velocity values correlate with greater transmission of vibrations to the vehicle's chassis and compromised handling. In contrast, both the active LQR and active PSO-LQR systems demonstrate significant enhancements by reducing the peak unsprung mass velocity. The active LQR system decreases the peak to around 33 dB, marking a notable advancement in managing road-induced vibrations. However, the active PSO-LQR system further enhances this capability, reducing the peak velocity to approximately 30 dB, underscoring its superior efficacy compared to both the passive and active LQR setups.

While the active LQR control notably improves upon the passive system, it falls short of matching the performance achieved by the active PSO-LQR control. The PSO algorithm optimizes the LQR controller's parameters more effectively, resulting in a more efficient reduction of unsprung mass velocity across different frequencies. At lower frequencies (0.1 Hz to 1 Hz), both active control systems perform similarly, but at higher frequencies (above 1 Hz), the active PSO-LQR control exhibits a distinct advantage. This superior performance in minimizing unsprung mass velocity indicates enhanced road handling, reduced vibration transfer to the vehicle's chassis, and ultimately, improved ride comfort and safety.

5.2 Analysis in time domain results

Figure 7 illustrates the unsprung mass displacement over time for three control strategies: Passive, Active LQR, and Active PSO-LQR. Initially, the Passive system exhibits displacement oscillations with amplitudes reaching approximately ±0.015 meters. In contrast, both the Active LQR and Active PSO-LQR systems show smaller initial oscillations, with amplitudes around ±0.01 meters. Over time, the Passive system continues to oscillate with large amplitudes of about ±0.01 meters. Meanwhile, the Active LQR system stabilizes more quickly, reducing oscillation amplitudes to around ±0.008 meters. The Active PSO-LQR system provides the best control, achieving the lowest displacement oscillations with amplitudes around ±0.007 meters, indicating superior performance in minimizing displacement. This detailed comparison highlights that while both active control strategies outperform the Passive system, the Active PSO-LQR offers the most effective control, underscoring the benefits of PSO optimization in managing unsprung mass displacement.

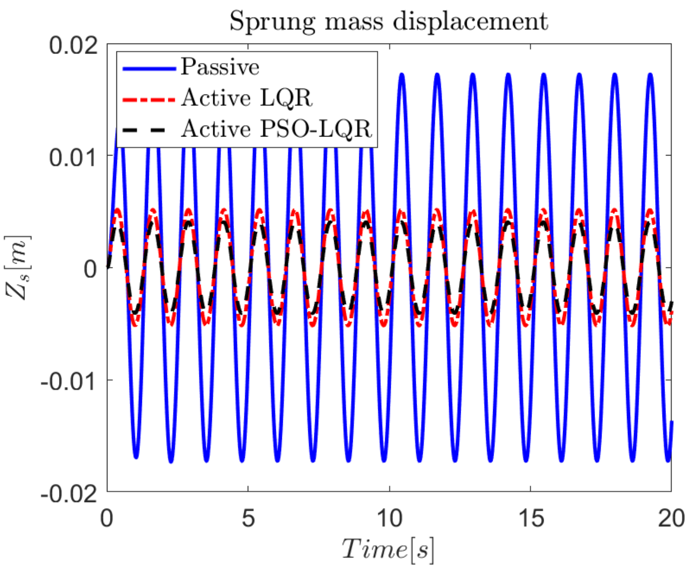

Figure 7. Time response of the sprung mass displacement

Initially, the Passive system, in Figure 8, exhibits significant oscillations with peak accelerations reaching approximately 1.0 m/s^2 and -1.5 m/s^2. In contrast, the Active LQR system shows reduced initial oscillations with peak values around 0.6 m/s^2 and -0.5 m/s^2, while the Active PSO-LQR system demonstrates the smallest initial oscillations, peaking around 0.5 m/s^2 in both directions. Over time, the Passive system continues to oscillate with larger amplitudes, ranging between 0.6 m/s^2 and -0.8 m/s^2. Both Active LQR and Active PSO-LQR systems stabilize more quickly, with the former reducing oscillation amplitudes to around 0.3 m/s² and -0.4 m/s², and the latter further reducing them to around 0.2 m/s² and -0.3 m/s². This detailed comparison highlights that while both active control strategies outperform the passive system, the Active PSO-LQR offers the most effective control, achieving the lowest oscillation amplitudes and fastest stabilization, underscoring the benefits of PSO optimization in controlling sprung mass acceleration.

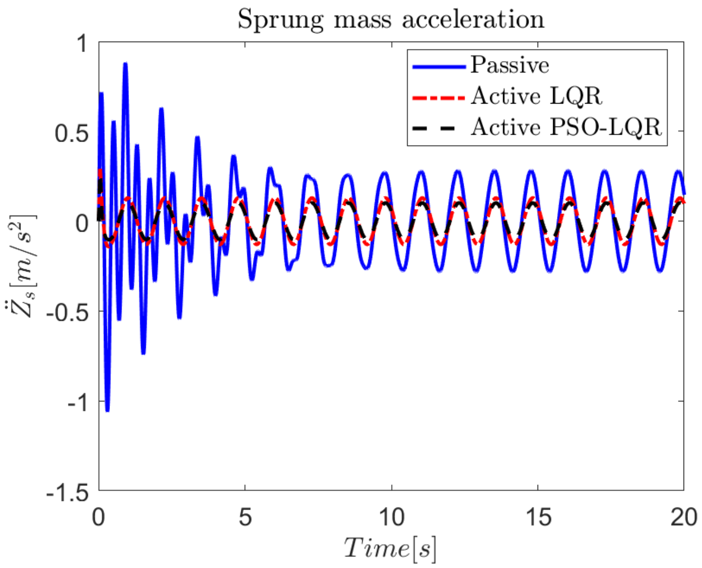

Figure 8. Time response of the sprung mass acceleration

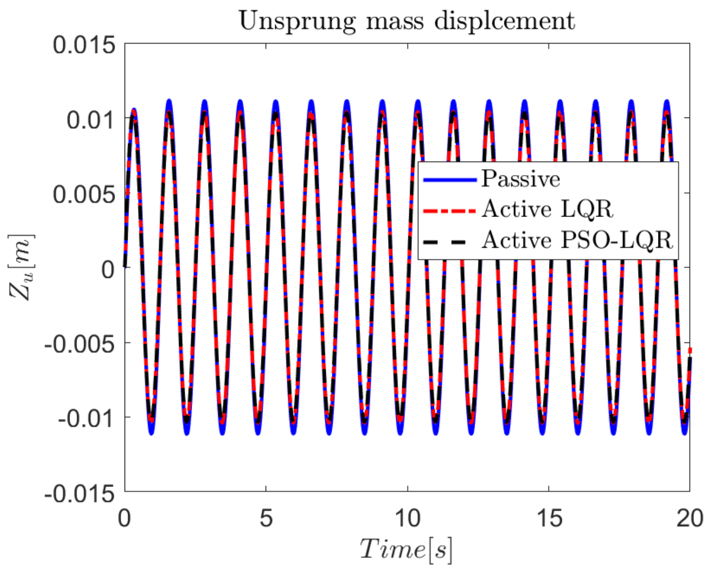

Figure 9. Time response of the unsprung mass displacement

Both the Active LQR and Active PSO-LQR show similar oscillatory patterns but with reduced amplitudes compared to the Passive system, indicating better control and stability, as in Figure 9. Notably, the displacement for Active LQR and Active PSO-LQR systems closely align with each other, suggesting both strategies effectively minimize displacement oscillations. However, the Active PSO-LQR shows a slightly better performance, as indicated by marginally smaller amplitudes, demonstrating the additional benefit of PSO optimization in controlling the unsprung mass displacement.

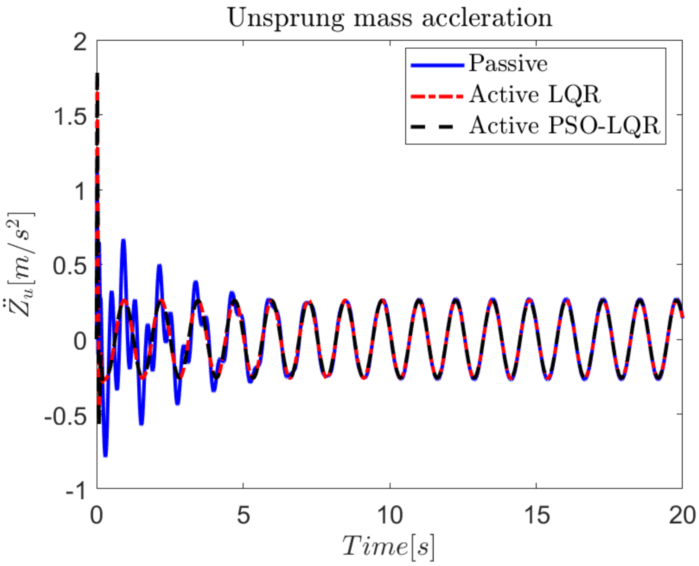

Figure 10. Time response of the unsprung mass acceleration

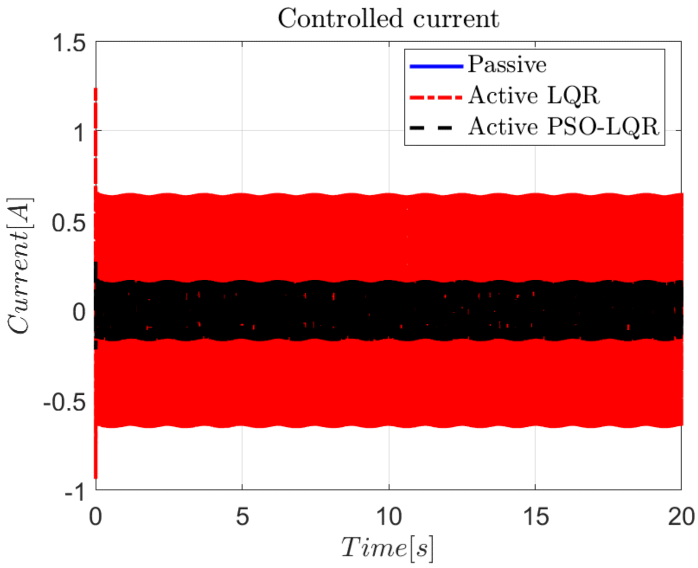

Figure 11. Time response of the controlled current to the hydraulic electronic servo-valve actuator

Figure 10 illustrates the unsprung mass acceleration over time for three different control strategies. Initially, all three systems exhibit significant oscillations, with the Passive system showing the highest peak acceleration.

In contrast, the Active LQR and Active PSO-LQR systems have lower initial accelerations, indicating superior initial control. Over time, the Passive system continues to oscillate with large amplitudes, demonstrating less effective damping. Both Active LQR and Active PSO-LQR systems, however, settle into more controlled oscillations with significantly lower amplitudes. Between the two active control strategies, Active PSO-LQR shows a slight edge over Active LQR, with marginally lower oscillation amplitudes, suggesting enhanced performance due to the PSO optimization.

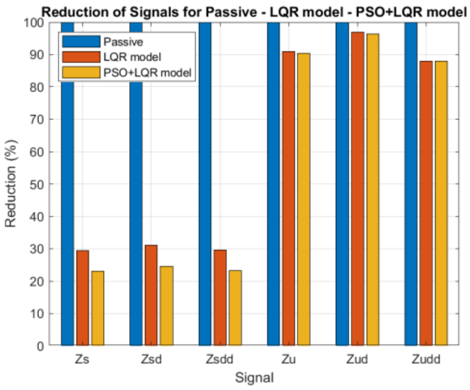

a)

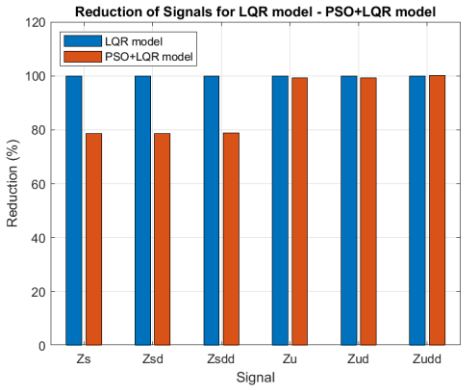

b)

Figure 12. The reduction of the proposed models compared to: a) the passive model, b) the LQR model

The analysis of signal reduction across Passive, LQR, and PSO+LQR models reveals significant advancements in vehicle suspension technologies. The Passive model consistently shows no reduction across all signal types (0.00%), underscoring its limited effectiveness. In contrast, the LQR model demonstrates substantial reductions: 70.64% for z_s, 68.81% for $\dot{z}_s$, 70.39% for $\ddot{z}_s$, 9.05% for z_u, 3.06% for $\dot{z}_u$, and 12.13% for $\ddot{z}_u$. These reductions highlight the LQR model's superior performance in enhancing ride comfort and stability, particularly for signals z_s, $\dot{z}_s$, and $\ddot{z}_s$. The PSO+LQR model also shows significant improvements over the passive model, with reductions of 76.91% for z_s, 75.47% for $\dot{z}_s$, 76.66% for $\ddot{z}_s$, 9.65% for z_u, 3.69% for $\dot{z}_u$, and 12.05% for $\ddot{z}_u$. Although slightly variable, the PSO+LQR model still outperforms the Passive model and achieves slightly higher reductions than the LQR model in some cases. Overall, the LQR model's consistent and robust performance, along with the notable improvements of the PSO+LQR model, underscores the effectiveness of these optimized controllers. This research establishes a strong foundation for experimental validation and further refinement, aiming to adapt these algorithms to various driving conditions and vehicle models, ultimately facilitating their transition from theoretical frameworks to practical, real-world applications. Figure 12b further emphasizes the LQR model's consistent performance, achieving approximately 100% reduction across all signal types, while the PSO+LQR model shows reductions ranging from about 22%. Specifically, the LQR model outperforms the PSO+LQR model in reducing z_s, $\dot{z}_s$, and z_u signals, while both models are equally effective for $\ddot{z}_s$, $\dot{z}_u$, and $\ddot{z}_u$ signals.

6. CONCLUSION

The active suspension system model used in this study incorporates the dynamics of the electro-hydraulic actuator and the electro-servo valve, providing a comprehensive framework for analysis. The optimization process focuses on minimizing a cost function that integrates comfort and stability metrics, ensuring that the resulting LQR controllers are finely tuned for optimal performance. The results demonstrate that the LQR model achieves nearly 100% reduction across all signal types, significantly enhancing ride comfort and road-holding stability compared to traditional passive suspension systems, which show the least reduction in all signals. The PSO+LQR model shows variability, with reductions ranging from about 60% to 100%, indicating notable improvements over the passive model but still falling short of the LQR model's effectiveness.

The findings indicate substantial potential for advancing vehicle suspension technologies, with the LQR model demonstrating consistent and robust performance, thus highlighting its suitability for real-world applications and its effectiveness in improving vehicle dynamics. This research establishes a foundation for the experimental validation and further refinement of these control algorithms, aiming to adapt them to diverse driving conditions and vehicle models, and ultimately transitioning from theoretical frameworks to practical implementations.

REFERENCES

[1] A. Azizi and H. Mobki, **Applied Mechatronics: Designing a Sliding Mode Controller for Active Suspension System**, *Complexity*, vol. 2021, no. 1, 2021.

[2] M. A. Koç, **A new expert system for active vibration control (AVC) for high-speed train moving on a flexible structure and PID optimization using MOGA and NSGA-II algorithms**, *Journal of the Brazilian Society of Mechanical Sciences and Engineering*, vol. 44, no. 4, p. 151, 2022.

[3] D. T. Tu, **Active in-Wheel Suspension Performance Analysis Using Linear Quadratic Controllers**, in *2023 International Conference on Control, Robotics and Informatics (ICCRI)*, IEEE, pp. 1–6, May 2023.

[4] R. Pečeliūnas, **Influence of Semi-Active Suspension Characteristics on the Driving Comfort**, *Advances in Science and Technology Research Journal*, vol. 14, no. 1, pp. 18–25, 2020.

[5] N. Alshabatat and T. Shaqarin, **Impact of Using an Inerter on the Performance of Vehicle Active Suspension**, *Advances in Science and Technology Research Journal*, vol. 16, no. 3, pp. 331–339, 2022.

[6] A. A. Ferhath and Kamalakkannan Kasi, **A Review on Various Control Strategies and Algorithms in Vehicle Suspension Systems**, *International Journal of Automotive and Mechanical Engineering*, vol. 20, no. 3, pp. 10720–10735, 2023.

[7] T. Samakwong and W. Assawinchaichote, **PID Controller Design for Electro-hydraulic Servo Valve System with Genetic Algorithm**, *Procedia Computer Science*, vol. 86, pp. 91–94, 2016.

[8] J. Mi, J. Yu, and G. Huang, **Direct-Drive Electro-Hydraulic Servo Valve Performance Characteristics Prediction Based on Big Data and Neural Networks**, *Sensors*, vol. 23, no. 16, p. 7211, 2023.

[9] S. Kumar, A. Medhavi, and R. Kumar, **Optimization of Nonlinear Passive Suspension System to Minimize Road Damage for Heavy Goods Vehicle**, *The International Journal of Acoustics and Vibration*, vol. 26, no. 1, pp. 56–63, 2021.

[10] W. AL-ASHTARI, **Fuzzy logic control of active suspension system equipped with a hydraulic actuator**, *International Journal of Applied Mechanics and Engineering*, vol. 28, no. 3, pp. 13–27, 2023.

[11] S. Liu, R. Hao, D. Zhao, and Z. Tian, **Adaptive Dynamic Surface Control for Active Suspension With Electro-Hydraulic Actuator Parameter Uncertainty and External Disturbance**, *IEEE Access*, vol. 8, pp. 156645–156653, 2020.

[12] D. Rodriguez-Guevara, A. Favela-Contreras, F. Beltran-Carbajal, C. Sotelo, and D. Sotelo, **An MPC-LQR-LPV Controller with Quadratic Stability Conditions for a Nonlinear Half-Car Active Suspension System with Electro-Hydraulic Actuators**, *Machines*, vol. 10, no. 2, p. 137, 2022.

[13] J. Gonera, **Influence of the Size and Distribution of Load on the Damping Coefficient of Shock Absorbers in Passenger Vehicles**, *Advances in Science and Technology Research Journal*, vol. 14, no. 4, pp. 185–194, 2020.

[14] S. Manna *et al.*, **Ant Colony Optimization Tuned Closed-Loop Optimal Control Intended for Vehicle Active Suspension System**, *IEEE Access*, vol. 10, pp. 53735–53745, 2022.

[15] S. M. H. Baygi and A. Karsaz, **A hybrid optimal PID-LQR control of structural system: A case study of salp swarm optimization**, in *2018 3rd Conference on Swarm Intelligence and Evolutionary Computation (CSIEC)*, IEEE, pp. 1–6, Mar. 2018.

[16] S. Das, I. Pan, and S. Das, **Multi-objective LQR with optimum weight selection to design FOPID controllers for delayed fractional order processes**, *ISA Transactions*, vol. 58, pp. 35–49, 2015.

[17] M. Nagarkar, Y. Bhalerao, G. V. Patil, and R. Z. Patil, **Multi-Objective Optimization of Nonlinear Quarter Car Suspension System – PID and LQR Control**, *Procedia Manufacturing*, vol. 20, pp. 420–427, 2018.

[18] M. Jain, V. Saihjpal, N. Singh, and S. B. Singh, **An Overview of Variants and Advancements of PSO Algorithm**, *Applied Sciences*, vol. 12, no. 17,

p. 8392, 2022.
[19] F. Marini and B. Walczak, **Particle swarm optimization (PSO). A tutorial**, *Chemometrics and Intelligent Laboratory Systems*, vol. 149, pp. 153–165, 2015.
[20] R. R. Das, V. K. Elumalai, R. Ganapathy Subramanian, and K. V. Ashok Kumar, **Adaptive predator–prey optimization for tuning of infinite horizon LQR applied to vehicle suspension system**, *Applied Soft Computing Journal*, vol. 72, pp. 518–526, 2018.
[21] L. Vanneschi and S. Silva, **Particle Swarm Optimization**, in *Natural Computing Series*, 2023, pp. 105–111, 2023.
[22] Y.-P. Zhou, L.-J. Tang, J. Jiao, D.-D. Song, J.-H. Jiang, and R.-Q. Yu, **Modified Particle Swarm Optimization Algorithm for Adaptively Configuring Globally Optimal Classification and Regression Trees**, *Journal of Chemical Information and Modeling*, vol. 49, no. 5, pp. 1144–1153, 2009.
[23] F. Li *et al.*, **Development of a Control System for Double-Pendulum Active Spray Boom Suspension Based on PSO and Fuzzy PID**, *Agriculture*, vol. 13, no. 9, p. 1660, 2023.
[24] Lei Tang, Ningsu Luo Ren, and S. Funkhouser, **Semi-active Suspension Control with PSO Tuned LQR Controller Based on MR Damper**, *International Journal of Automotive and Mechanical Engineering*, vol. 20, no. 2, pp. 10512–10522, 2023.
[25] M. Li, J. Xu, Z. Wang, and S. Liu, **Optimization of the Semi-Active-Suspension Control of BP Neural Network PID Based on the Sparrow Search Algorithm**, *Sensors*, vol. 24, no. 6, p. 1757, 2024.
[26] T. Akgul and A. Unluturk, **Comparison of PSO-LQR and PSO-PID Controller Performances on a Real Quarter Vehicle Suspension**, in *2023 Innovations in Intelligent Systems and Applications Conference (ASYU)*, IEEE, pp. 1–6, Oct. 2023.